THE JOURNAL OF PHYSICAL CHEMISTRY Letters

Letter

Cite This: J. Phys. Chem. Lett. 2018, 9, 6991−6998

pubs.acs.org/JPCL

Does Local Structure Bias How a Crystal Nucleus Evolves?

Kyle Wm. Hall,[†,‡,#] Zhengcai Zhang,[†,§] Christian J. Burnham,[∥] Guang-Jun Guo,[§,⊥] Sheelagh Carpendale,[‡] Niall J. English,[∥] and Peter G. Kusalik*[,†]

[†]Department of Chemistry, University of Calgary, Calgary, Alberta T2N 1N4, Canada

[‡]Department of Computer Science, University of Calgary, Calgary, Alberta T2N 1N4, Canada

[§]Key Laboratory of Earth and Planetary Physics, Institute of Geology and Geophysics, Chinese Academy of Sciences, Beijing 100029, China

[∥]School of Chemical and Bioprocess Engineering, University College Dublin, Belfield, Dublin 4, Ireland

[⊥]College of Earth Science, University of Chinese Academy of Sciences, Beijing 100049, China

Supporting Information

ABSTRACT: The broad scientific and technological importance of crystallization has led to significant research probing and rationalizing crystal nucleation processes. Previous work has generally neglected the possibility of the molecular-level dynamics of individual crystal nuclei coupling to local structures. However, recent experimental work has conjectured that this can occur. Therefore, to address a deficiency in scientific understanding of crystallization, we have probed the nucleation of prototypical single and multicomponent crystals (specifically, ice and mixed gas hydrates). We establish that local structures can bias the evolution of nascent crystal phases on a nanosecond time scale by, for example, promoting the appearance or disappearance of specific crystal motifs and thus reveal a new facet of crystallization behavior. Moreover, we demonstrate structural biases are likely present during crystallization processes beyond ice and gas hydrate formation. Structurally biased dynamics are a lens for understanding existing computational and experimental results while pointing to future opportunities.

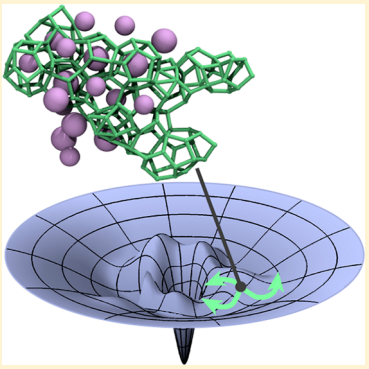

Crystallization is ubiquitous and highly relevant to many scientific and technological applications (e.g., bone formation, pharmaceuticals, meteorology, and metallurgy). For many applications, either promoting or inhibiting crystallization can be advantageous. Molecular-level understanding of crystallization will help advance attempts to control, probe, and rationalize crystallization behavior. However, as highlighted by a recent review,[1] scientific understanding of crystal nucleation—the emergence of an initial ordered structure (i.e., a nucleus)—remains incomplete with key outstanding questions. Debenedetti has discussed how prevailing nucleation theories[2] typically invoke nuclei distributions and diffusive behaviors to rationalize nucleation phenomenology,[3] rather than describing specific microscopic events contributing to the evolution of an individual nucleus. Previous work also assumes that successive particle attachment and detachment events for a crystal nucleus are uncorrelated[1] and that their associated rates, though dependent on nucleus size, are agnostic to nucleus structure.[3,4] These aforementioned assumptions are rarely questioned, and many studies implicitly accept them by invoking classical nucleation theory.[5−7] In contrast, it has been shown that the continuous macroscopic nature of classical nucleation theory does not capture the thermodynamics of small nuclei.[8] Moreover, the molecular-level shortcomings of prevailing ideas about crystal nucleation are becoming increasingly clear as highlighted by work on disparate processes (e.g., protein[9] and diamond[10] crystallization). Is not likely that the molecular-level details of a nucleus's local structure and its surrounding environment could give rise to richer dynamical behaviors than those captured by prevailing perspectives on crystallization? Previous work has essentially not considered this possibility. In contrast, recent experimental work[11] claims, though does not substantiate, that the occurrence of metastable low-symmetry phases in diblock copolymer systems arises from local structure guiding nucleation processes. Here, we confirm that local structures can influence how a crystal nucleus evolves. More specifically, we have discovered that individual nuclei can exhibit markedly differing biased behaviors on nanosecond time scales and that local structural environments can predispose comparably sized nuclei to grow or melt in specific ways. Our results, in conjunction with a careful analysis of existing results,[12−20] reveal that structurally biased dynamics are likely a general feature of nucleation.

It remains experimentally challenging to study crystal nucleation at the molecular level,[1] and understanding experimental results is impeded by difficulties observing nuclei during crystallization in molecular systems.[21] Simulations allow for detailed examination of crystal nuclei, which can reveal

Received: October 9, 2018
Accepted: November 28, 2018
Published: November 28, 2018

DOI: 10.1021/acs.jpclett.8b03115
J. Phys. Chem. Lett. 2018, 9, 6991−6998

unique insights[22,23] and enable experimental interpretation.[21] Direct molecular dynamics (MD) simulations are well-suited for studying the influences of local structure on dynamics during nucleation because direct (so-called brute-force) MD simulations do not bias the investigation of nucleation behavior.[1] However, comparatively few nucleation processes are amenable to direct MD simulations (exceptions include nucleation in colloidal and atomic systems).[1]

We have chosen to probe the nucleation of prototypical single-component and multicomponent small-molecule crystals that are amenable to in silico investigations using direct MD simulations. For single-component nucleation, we have probed ice nucleation, given its ubiquitous relevance (e.g., to biology and climate modeling). To probe multicomponent nucleation, gas hydrate formation has been studied in a $CH_4/H_2S/H_2O$ system. Gas hydrates are crystals in which water molecules form host lattices of polyhedral hydrogen-bond cages that enclathrate small gas guest molecules (e.g., methane). Gas hydrates are a major flow-assurance concern in pipelines,[24] a potential strategy for hydrogen storage,[25,26] and a contributor to the global methane cycle.[27,28] We have performed extensive direct MD simulations of hydrate and ice nucleation at atomistic and picosecond resolutions, using the isoconfigurational-ensemble approach,[29] to resolve the impact of local structure on dynamics. For our simulations, we have used previously established models and methods, so we only briefly introduce the isoconfigurational ensemble approach below while providing all additional methodological details in the Supporting Information.

In this study, an isoconfigurational ensemble[29] is a swarm of 4 ns long simulation trajectories with a common starting configuration (initial structural arrangement of particles) but differing velocity assignments as achieved through particle-velocity randomization (see section 1 in the Supporting Information for methodological details and Figure 1). If the starting configuration's structure does not influence the system's subsequent dynamics, then the ensemble of trajectories should not exhibit correlated behavior as they evolve. In contrast, through isoconfigurational ensembles, previous studies have demonstrated that local structure impacts behavior within glasses[29,30] and affects crystal growth at ice−water interfaces.[31] Here, we present results from four isoconfigurational ensembles for hydrate nucleation (ensembles 1−4) and four for ice nucleation (ensembles 5−8). Results from two additional hydrate ensembles (ensembles 9 and 10) are provided in the Supporting Information and referenced as needed.

Recent work[32,33] has revealed that both hydrate and ice nucleation exhibit comparatively flat free-energy profiles near their barriers (i.e., near the "critical" nucleus). Therefore, near-critical nuclei (whether pre- or postcritical) should exhibit underlying kinetics comparable to those of critical nuclei, and their behavior should be largely diffusive according to classical nucleation theory. The nuclei used to launch our isoconfigurational ensembles are near critical (i.e., containing trajectories exhibiting both growth and melting behavior). We classify ensembles by their predisposition toward growth or melting. At longer times, ensembles 1−4 are predisposed toward growth, while ensembles 5−10 tend toward melting. Both sets of ensembles yield comparable insights, so our conclusions are relevant to nuclei near nucleation free-energy barriers, including critical nuclei.

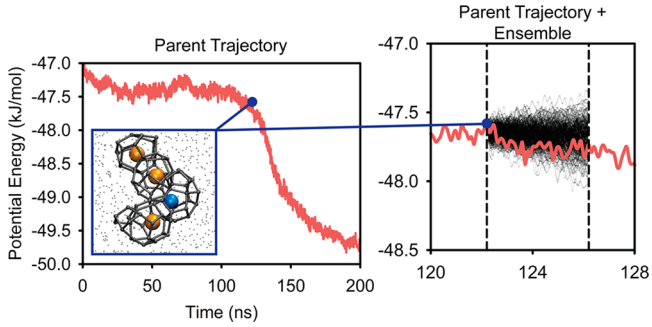

Figure 1. Generating an isoconfigurational ensemble. Left: the potential-energy curve of a hydrate-nucleation MD trajectory for a $CH_4/H_2S/H_2O$ system. The blue point indicates the location of the starting configuration used to generate the isoconfigurational ensemble. Water cages are basic structural motifs of hydrates; we analyzed both complete and face-saturated incomplete cages[34,35] using a modified version of the FSICA approach.[35] The inset's gray tubes connect the oxygen atoms of the water molecules composing the starting configuration's cluster of cages. Enclathrated H_2S and CH_4 molecules are represented as orange and blue spheres, respectively. The gray points correspond to the oxygen atoms of the surrounding water molecules. Right: an overlay of the potential-energy curves for the trajectories composing the resulting isoconfigurational ensemble (as shown in black) and the potential-energy curve of the parent trajectory (as shown in red). The variation in the curves highlights how the parent trajectory is just one sampling of how the starting configuration can evolve. Moreover, some trajectories within the ensemble exhibit increasing potential energies, emphasizing that the nucleus has a nonzero probability of displaying melting behavior during the 4 ns window. The dashed vertical lines indicate the start and end of the isoconfigurational ensemble's 4 ns time window. Henceforth, stated times correspond to times elapsed since the start of an isoconfigurational ensemble unless stated otherwise.

Through careful analysis of the behavior exhibited by ensembles 1−10, we have discovered that nuclei can be predisposed to evolve in specific ways at shorter times that are distinct from their longer-time behaviors. For example, for ensembles 1−4, each ensemble's constituent trajectories realized, on average, net hydrate formation during the 4 ns window according to order parameters designed to monitor hydrate formation (e.g., number of guest-filled water cages and MCG3 cluster size[36] as shown in Figure 2A,B). However, ensembles 1−4 also exhibit strikingly different shorter-time behaviors. In Figure 2A, ensemble 3 exhibits a short-lived enhanced propensity to add singly occupied cages compared to other ensembles, while ensemble 2 exhibits a short-lived melting tendency. Moreover, although longer-time behaviors of singly occupied cage populations and MCG3 cluster sizes are qualitatively comparable for a given ensemble, their shorter-time behaviors can differ (see ensemble 3 in Figure 2A,B). The discrepancies between the two metrics highlight how they probe somewhat different facets of hydrate nucleation. Visual analysis of each ensemble's starting configuration similarly reveals that each configuration's largest cluster of cages and largest MCG3 cluster are overlapping, yet distinct, sets of particles (see Figure S12). However, the cage and MCG3 metrics agree that the isoconfigurational ensembles can exhibit distinct shorter-time behavior, a distinction also captured by dodecahedral-cage populations.

Dodecahedral cages are a structural component of gas hydrates.[37] Previous work has demonstrated that these cages

DOI: 10.1021/acs.jpclett.8b03115
J. Phys. Chem. Lett. 2018, 9, 6991−6998

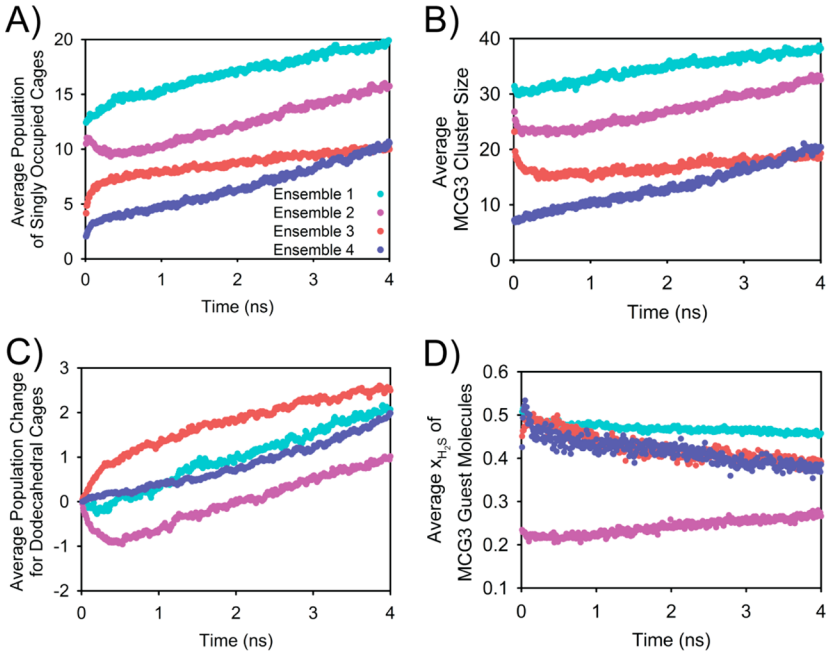

Figure 2. Property evolution for hydrate-nucleation ensembles 1−4 as averaged across their constituent trajectories. (A) The evolution of average populations of singly occupied water cages. For panel A and the subsequent panels, the standard error bars associated with the ensemble averages are comparable to the symbol sizes used to represent the data. (B) The evolution of average MCG3 cluster sizes, which have been previously used to monitor hydrate formation.[36] (C) Change in average populations of dodecahedral (5^{12}) cages relative to the number of dodecahedral cages in each ensemble's starting configuration. (D) The evolution of average H_2S mole fraction for the MCG3 clusters within each ensemble's constituent trajectories. The mole fractions consider only the guest molecules (i.e., CH_4 and H_2S) participating in the MCG3 clusters. Panels B−D use the same color scheme as panel A.

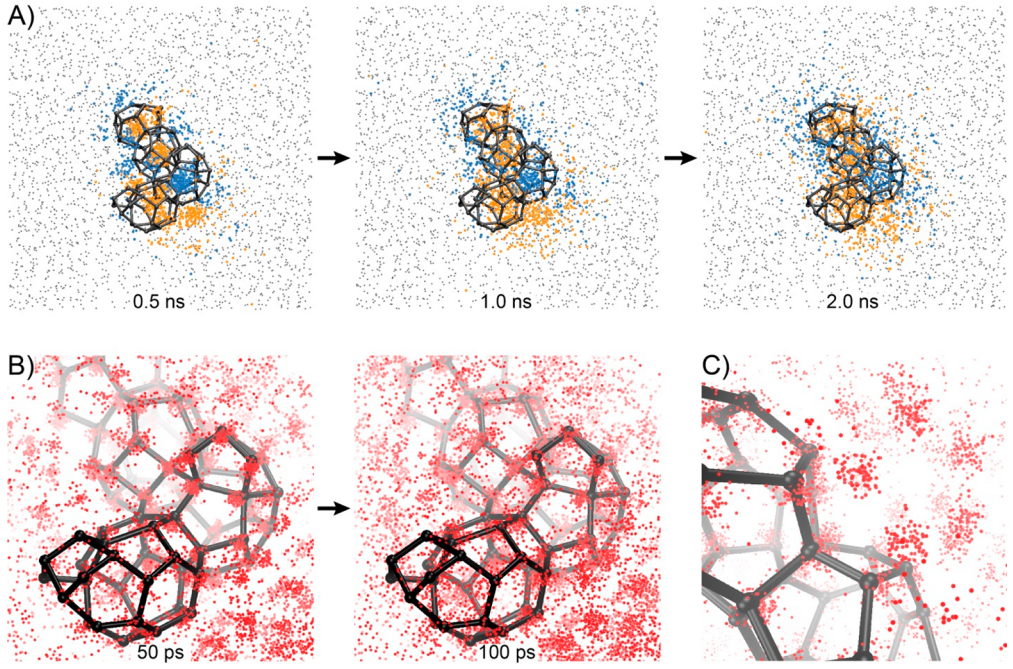

Figure 3. Structural correlations among ensemble 3's constituent trajectories, which were launched from the configuration in Figure 1. (A) Spatial correlations in the guest molecules enclathrated by the ensemble's trajectories. Blue and orange points correspond to the CH_4 and H_2S molecules enclathrated by the largest clusters of cages in the constituent trajectories at the specified times. The gray tubes correspond to the occupied water cages in the ensemble's starting configuration (i.e., the cluster of cages in Figure 1), while gray points show the positions of the oxygen atoms of the surrounding water molecules. (B) Spatial correlations in the cage-forming water molecules. As in panel A, gray tubes indicate the occupied cages in the initial configuration. The red points are an overlay of the oxygen-atom positions for those H_2O molecules composing each trajectory's largest cluster of cages at 50 and 100 ps. (C) An oblique view of the overlaid configurations in the right image of panel B. Panels B and C leverage depth culling.

DOI: 10.1021/acs.jpclett.8b03115
J. Phys. Chem. Lett. 2018, 9, 6991−6998

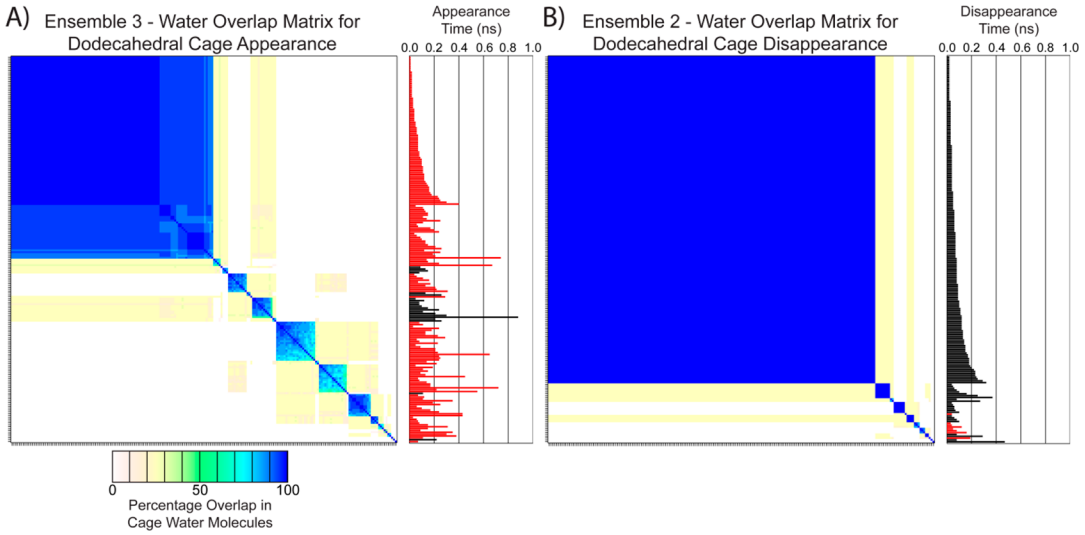

Figure 4. Correlations in cage dynamics among an isoconfigurational ensemble's trajectories. (A) The water overlap matrix for the first dodecahedral cages appearing in ensemble 3's trajectories. The ensemble's starting configuration provides a unique index of the system's water molecules. We extracted the indices of the water molecules that form the first dodecahedral cage in each trajectory. For each pair of trajectories, the percentage of H_2O molecules common to their first dodecahedral cages was calculated according to the extracted indices and stored as a matrix. Inspired by and using as a basis hierarchical clustering,[44] we performed cluster analysis, a type of machine learning, on the resultant matrix to detect groups of trajectories with overlapping sets of water indices for their first dodecahedral cages (see section 1.2.7 in the Supporting Information for more information). The matrix was sorted according to the cluster-analysis results and colored using the ramp at the bottom of panel A. If the initial structure used to generate the trajectories did not influence their subsequent dynamics, correlations between trajectories would be minimal and high-overlap blue regions would be small. The ticks at the edge of the matrix mark each trajectory. The bar graph to the right indicates when the cage corresponding to a matrix row appears in its corresponding trajectory. Red and black bars indicate H_2S and CH_4-filled cages. (B) The water-overlap matrix for the first dodecahedral cages to disappear in ensemble 2's trajectories. The matrix has been constructed the same way as panel A, but using water indices of the first dodecahedral cages to disappear in ensemble 2's trajectories. The bar graph to the right indicates when the cage corresponding to a matrix row disappears in it corresponding trajectory. Panel B uses the same colors as panel A.

are important to the early stage formation of CH_4, H_2S, and mixed CH_4/H_2S hydrates.[38−43] As can be seen in Figure 2C, ensemble 2's trajectories display a strong initial propensity to lose a dodecahedral cage while ensemble 3's constituent trajectories show strong propensity to gain a dodecahedral cage. Given that dodecahedral cages consist of hydrogen-bonded five-membered water rings, we extracted the time evolution of each ensemble's average population of water pentamers as confirmatory analysis (see section 1.2.6 in the Supporting Information). Changes in ensemble-averaged pentamer populations (see section 2.1 in the Supporting Information) are generally in accord with the dodecahedral-cage behaviors in Figure 2C, reinforcing that the ensembles display differing behaviors, particularly at short times. Therefore, the conclusion that the ensembles, and hence nuclei, exhibit distinct shorter-time behavior is robust with respect to alternative hydrate-nucleation metrics. Furthermore, distinctions between shorter and longer-time behaviors are also robust with respect to thermodynamic-ensemble choices (see section 2.2 in the Supporting Information).

Given that each isoconfigurational ensemble's constituent trajectories were created through velocity randomization, the differing shorter-time behaviors of the ensembles must arise from each ensemble's starting structure causing correlations in how each ensemble's constituent trajectories evolve. Consistent with this, ensemble 3's trajectories exhibit structural correlations in the vicinity of the growing hydrate nucleus. Strong guest-species specificity is evident at positions coinciding with enclathrated guest species in the ensemble's starting configuration (compare Figure 3A to Figure 1). However, guest specificity also extends beyond the initial cage set, and the trajectories still exhibit some extended correlated behavior even after 2 ns (see Figure 3A). In fact, ensembles 1−4 are apparently compositionally distinct even after 4 ns (see Figure 2D). Ensemble 3's trajectories also exhibit structural correlations in terms of water-molecule positions (see Figure 3B), and these correlations also extend beyond the ensemble's initial cluster of cages (see Figure 3C). Given that there are structural correlations among the trajectories, it is reasonable to expect that an ensemble's trajectories are also correlated in terms of how their nuclei evolve with respect to their cage additions, for example.

To probe for behavioral correlations among each ensemble's constituent trajectories, we extracted the percentages of water molecules common to cages appearing and disappearing within an ensemble's trajectories and used machine learning and visualization to produce symmetric overlap matrices from this data (see the caption for Figure 4A and the Supporting Information). These matrices reveal that groups of water molecules within an ensemble's starting configuration can be strongly predisposed to undergo particular structural rearrangements. For example, ensemble 3's trajectories have a strong tendency for their first dodecahedral cages to form primarily from a few specific groups of water molecules (e.g., see the large blue region in Figure 4A). Moreover, trajectories with strong overlap in their first dodecahedral cages also exhibit strong correlations in the guest species occupying their respective cages, as can be seen by comparing each blue region in Figure 4A with the color of the bars at the right of the panel. However, trajectories with strong overlap do not exhibit strong temporal correspondence in cage appearances. Their cages appear over several hundred picoseconds. Therefore, the local

DOI: 10.1021/acs.jpclett.8b03115
J. Phys. Chem. Lett. 2018, 9, 6991−6998

structural milieux can influence cage dynamics for hundreds of picoseconds. Ensemble 2, whose starting configuration contained three dodecahedral cages, exhibits similar phenomenology in terms of disappearing dodecahedral cages. The overlap matrix for the first dodecahedral cages to disappear from ensemble 2's trajectories shows that the majority of the trajectories lose a methane-filled dodecahedral cage composed of specific water molecules (see Figure 4B). Ensembles 1 and 4, which lack strong initial propensities to either add or lose dodecahedral cages, also exhibit correlated behavior between their trajectories (see section 2.3 in the Supporting Information where higher-resolution versions of the matrices in Figure 4 are also provided). A nucleus's structure and its local environment can thus impact the shorter-time evolution and dynamics of that nucleus.

Individual gas hydrate nuclei apparently do not evolve through successive independent particle attachment and detachment events with diffusive-like behavior. Rather, existing structures predispose a nucleus to evolve in certain ways, particularly at shorter times. Moreover, structural biases can impact system behavior and cage dynamics over hundreds of picoseconds (see Figure 4), and compositional differences can persist over nanoseconds (Figure 2D). Although ensembles 1−4 are predisposed to growth, we obtained comparable results for hydrate nuclei destined to melt (see section 2.4 in the Supporting Information).

To establish that structural biases can occur during other nucleation processes, we also probed ice nucleation. More specifically, we generated isoconfigurational ensembles for ice nuclei by leveraging the configurations from the forward-flux sampling in ref 45 (see section 1.3 in the Supporting Information). For the trajectories composing each ensemble, we extracted the time evolution of their largest clusters of diamond and hexagonal cages using a modified version of the FSICA approach[35] (see section 1.3.3 in the Supporting Information). Though the ensembles and hence their starting nuclei are inclined toward dissociation as evidenced by decreasing average cage-cluster sizes in Figure 5A, the ensembles do display differing shorter and longer time behaviors. In particular, ensemble 8 shows a predisposition toward shorter-time growth, despite its longer-time melting behavior as can be seen in Figure 5A, and ensemble 8's trajectories exhibit appreciable structural correlations (see Figure 5B). Ensembles 5−7 exhibit shorter-time melting. As with hydrates, local structure can bias ice-nucleation dynamics for hundreds of picoseconds.

On the basis of the crystallization literature, structurally biased dynamics are likely occurring during crystallization processes beyond ice and hydrate nucleation. For instance, a recent review[16] emphasizes that crystallization tends to take place in regions with enhanced "orientational order" and points to both computational and experimental studies probing various systems (e.g., colloidal systems[12]). Recent work[20] on homogeneous crystal nucleation in glass-forming metal alloys demonstrates that icosahedral short-range order can impede crystal nucleus development, yielding nonmonotic temperature dependence of crystallization free-energy barriers. For heterogeneous nucleation, foreign substances might either promote or inhibit crystallization in metastable solutions and melts through perturbations to local configurations and their structurally biased dynamics. This conjecture is supported by previous work on heterogeneous ice nucleation demonstrating that surfaces can promote nucleation via aqueous-phase

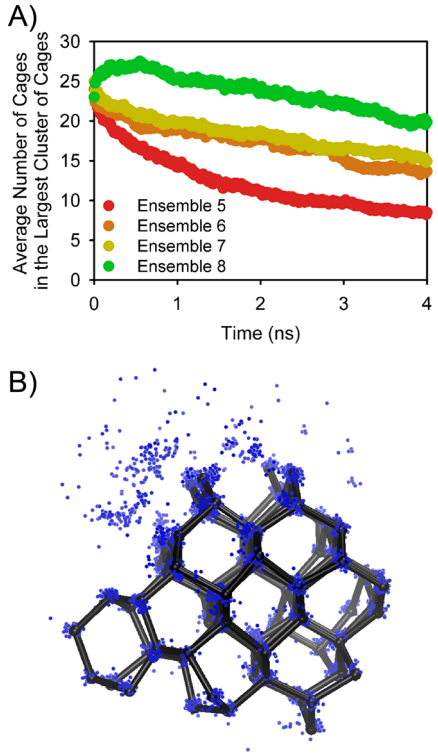

Figure 5. Results for ice isoconfigurational ensembles. (A) Evolution of the size of each ensemble's largest cluster of diamond and hexagonal cages as averaged across its constituent trajectories. (B) Structural correlation in ensemble 8's trajectories. Black tubes correspond to the largest cluster of diamond and hexagonal water cages in the ensemble's starting configuration. The blue points are an overlay of the oxygen-atom positions for the H_2O molecules participating in the largest clusters of cages within the ensemble's constituent trajectories 200 ps after the start of the ensemble. Only around the upper portion of the initial cluster of cages is there a substantial protrusion of blue dots, indicating that the ensemble's constituent trajectories do not uniformly add cages across the surface of the cluster.

structuring[13−15,17,18] and that minor variations in substrate structure can substantially impact a substrate's ability to promote ice nucleation.[17] Surfaces and surface geometries can also induce polymorph selection.[13,17,18] For example, during surface-induced heterogeneous crystal nucleation in high-volume fraction colloidal systems, supercooled-liquid preordering can dictate the final states of these systems.[19] Similarly, work on protein crystallization has demonstrated that polymorph selection occurs during the very early stages of ordering and stems from specific structural motifs.[46] Therefore, structurally biased dynamics are probably relevant to both homogeneous and heterogeneous nucleation, as well as polymorph selection, in disparate systems. Further investigation is needed.

Given that simulation studies aim to probe crystallization at the molecular level and short time scales (perhaps picoseconds), structurally biased dynamics also provide new perspectives on common computational strategies. For example, in the forward-flux paradigm,[47,48] the pathway between the solution and crystal macrostates is probed by essentially using sequential series of isoconfigurational ensembles and selectively evolving some of the constituent trajectories. Forward-flux studies can thus involve a small number of configurations yielding the majority of trajectories

DOI: 10.1021/acs.jpclett.8b03115
J. Phys. Chem. Lett. 2018, 9, 6991−6998

connecting the solution and crystal states[49,50] and short simulations (e.g., tens to hundreds of picoseconds).[45] In such scenarios, the forward-flux protocol could be coupling to structurally biased dynamics early on in the crystallization process and hence not provide a comprehensive perspective on crystal nucleation. Consequently, care is needed to ensure that results from a set of forward-flux simulations are representative of the nucleation process of interest and not strongly influenced by small numbers of ordered structures and their associated dynamics. Recently, Haji-Akbari[51] introduced an improved variant of forward-flux sampling in which transition probabilities between nucleus sizes are determined in a history-dependent fashion. More specifically, the transition probability from a nucleus of size n to $n + 1$ depends on how the system arrived at the n-size nucleus; we propose that the need for such algorithmic innovation arises from structurally biased dynamics.

Structurally biased dynamics are relevant to both explaining previous experimental work and inspiring future studies. Recent ice-nucleation experiments in "no man's land" considered conditions where nucleation and structural relaxation rates become comparable,[52−55] with large differences between different experiments being noted but unexplained.[53,55] The different system-preparation protocols used in the aforementioned studies likely result in metastable liquids with somewhat different local structures, and these structural differences are then manifested as differences in observed nucleation rates via structurally biased dynamics. In terms of future work, our demonstration that crystal-promoting and inhibiting local structures can arise during nucleation affords the exciting possibility of pinpointing specific local structures that either enhance or inhibit the formation of order (or perhaps polymorph selection) during nucleation processes and leveraging this knowledge to design crystallization promoters and inhibitors systematically. Such a reality is close at hand. Recently, Gebbie et al.[10] experimentally prepared nucleus precursors for diamond crystallization from plasma-enhanced chemical vapor deposition and observed that isomeric precursor structures can have differing nucleation rates. The challenge for future work is to rationally design precursors to, for example, enhance nucleation rates; such work has the potential for broad impact.

In order to exploit structurally biased dynamics fully, their microscopic origins need to be characterized. Such work will require detailed characterizations of local nucleus structure, interfacial motifs, and nearby liquid regions in terms of both properties (e.g., symmetries and network topologies) and lifetimes. The need to characterize lifetimes arises from the fact that the time scales of structural biases are not necessarily well-captured by average molecular-relaxation metrics (see section 2.5 in the Supporting Information). As a forerunner to characterizing the origins of structurally biased dynamics, we anticipate the need for careful comparison and refinement of existing order parameters; see section 2.6 in the Supporting Information for a discussion of this point based on preliminary analysis of our gas hydrate and ice-nucleation simulations. We are currently undertaking a detailed study for gas hydrate and ice nucleation to elucidate the origins of structurally biased dynamics.

Structurally biased dynamics are consistent with recent work probing the rugged funnel-shaped potential-energy landscapes associated with crystal nucleation.[43] During nucleation in a liquid, a system progresses from an initial high-energy, high-entropy liquid state (i.e., the broad mouth of the funnel) to a low-energy, low-entropy crystalline state (i.e., its narrow bottom). Because the landscape is locally rugged with local minima and maxima, the system must navigate according to its thermal energy as it descends further into the funnel. Consequently, probabilities associated with the system evolving from its current configuration to those nearby will be different. If transitioning to more probable configurations involves common structural rearrangements (e.g., dissolution of a defective interfacial structure), then the system will be predisposed to undergoing those structural rearrangements. In turn, while an order parameter, such as nucleus size, may serve as a proxy for relative thermodynamic stability (i.e., how far the system is down the funnel), it might not be a reliable indicator of a nucleus's shorter-time dynamical predispositions (i.e., how the system explores the funnel's local topology). At longer times, structurally biased behaviors are reduced because the system has sufficient time to explore larger portions of its energy landscape, mitigating local-topology effects.

Although structurally biased dynamics are conceptually consistent with rugged funnel-shaped potential-energy landscapes and previous work[11] has conjectured that structurally biased dynamics are operative during crystallization processes, no previous study has explicitly demonstrated their existence and impact on crystal nucleation. On the basis of results presented herein, we have demonstrated that structurally biased dynamics do exist. Structurally biased dynamics constitute a new facet of crystallization phenomenology that is relevant to both experiments and simulations on crystallization phenomena ranging from homogeneous nucleation through to polymorph selection, while also affording new perspectives on existing results and future opportunities. While this Letter was under review, Kumar et al.[56] published a detailed study demonstrating that metastable mesophases can facilitate and guide zeolite crystallization processes; we interpret this behavior as yet another manifestation of structurally biased dynamics that demonstrates the potential to exploit structurally biased dynamics to tailor materials.

■ ASSOCIATED CONTENT

Supporting Information

The Supporting Information is available free of charge on the ACS Publications website at DOI: 10.1021/acs.jpclett.8b03115.

Methodological and analysis details, supplementary figures and analysis, and supplementary discussion (PDF)

■ AUTHOR INFORMATION

Corresponding Author

*E-mail: pkusalik@ucalgary.ca. Tel: +1 403-220-6244.

ORCID

Christian J. Burnham: 0000-0001-5574-4339
Guang-Jun Guo: 0000-0003-4822-3863
Niall J. English: 0000-0002-8460-3540
Peter G. Kusalik: 0000-0001-6270-663X

Present Address

#K.W.H.: Institute for Computational Molecular Science and Department of Chemistry, Temple University, Philadelphia, PA 19122.

DOI: 10.1021/acs.jpclett.8b03115
J. Phys. Chem. Lett. 2018, 9, 6991−6998

Notes

The authors declare no competing financial interest.

■ ACKNOWLEDGMENTS

The authors thank the following: Alberta Innovates − Technology Futures (AITF), Canadian Foundation for Innovation (CFI), Compute Canada, Ireland-Canada University Foundation (especially James Flaherty program), Natural Sciences and Engineering Research Council of Canada (RGPIN-2016-03845), National Natural Science Foundation of China (Grant Nos. 41602038 and 41372059), Science Foundation Ireland (SFI/15/ERC/I3142), SMART Technologies, the NSERC Vanier CGS Program, and the University of Calgary. P.G.K. acknowledges a Wenner-Gren Foundation Fellowship. The authors also thank Amir Haji-Akbari and Pablo G. Debenedetti for providing configurations of water systems containing ice nuclei.

■ REFERENCES

(1) Sosso, G. C.; Chen, J.; Cox, S. J.; Fitzner, M.; Pedevilla, P.; Zen, A.; Michaelides, A. Crystal Nucleation in Liquids: Open Questions and Future Challenges in Molecular Dynamics Simulations. *Chem. Rev.* **2016**, *116*, 7078−7116.
(2) Debenedetti, P. G. *Metastable Liquids: Concepts and Principles*; Princeton University Press: Princeton, NJ, 1996; pp 147−199.
(3) Turnbull, D.; Fisher, J. C. Rate of Nucleation in Condensed Systems. *J. Chem. Phys.* **1949**, *17*, 71−73.
(4) Auer, S.; Frenkel, D. Prediction of Absolute Crystal-Nucleation Rate in Hard-Sphere Colloids. *Nature* **2001**, *409*, 1020−1023.
(5) Knott, B. C.; Molinero, V.; Doherty, M. F.; Peters, B. Homogeneous Nucleation of Methane Hydrates: Unrealistic under Realistic Conditions. *J. Am. Chem. Soc.* **2012**, *134*, 19544−19547.
(6) Sanz, E.; Vega, C.; Espinosa, J. R.; Caballero-Bernal, R.; Abascal, J. L. F.; Valeriani, C. Homogeneous Ice Nucleation at Moderate Supercooling from Molecular Simulation. *J. Am. Chem. Soc.* **2013**, *135*, 15008−15017.
(7) Cabriolu, R.; Li, T. Ice Nucleation on Carbon Surface Supports the Classical Theory of Heterogeneous Nucleation. *Phys. Rev. E* **2015**, *91*, 052402.
(8) Milchev, A. Electrochemical Phase Formation on a Foreign Substrate − Basic Theoretical Concepts and Some Experimental Results. *Contemp. Phys.* **1991**, *32*, 321−332.
(9) Yau, S. T.; Vekilov, P. G. Quasi-Planar Nucleus Structure in Apoferritin Crystallization. *Nature* **2000**, *406*, 494−497.
(10) Gebbie, M. A.; Ishiwata, H.; McQuade, P. J.; Petrak, V.; Taylor, A.; Freiwald, C.; Dahl, J. E.; Carlson, R. M. K.; Fokin, A. A.; Schreiner, P. R.; et al. Experimental Measurement of the Diamond Nucleation Landscape Reveals Classical and Nonclassical Features. *Proc. Natl. Acad. Sci. U. S. A.* **2018**, *115*, 8284−8289.
(11) Kim, K.; Schulze, M. W.; Arora, A.; Lewis, R. M.; Hillmyer, M. A.; Dorfman, K. D.; Bates, F. S. Thermal Processing of Diblock Copolymer Melts Mimics Metallurgy. *Science* **2017**, *356*, 520−523.
(12) Tan, P.; Xu, N.; Xu, L. Visualizing Kinetic Pathways of Homogeneous Nucleation in Colloidal Crystallization. *Nat. Phys.* **2014**, *10*, 73−79.
(13) Zielke, S. A.; Bertram, A. K.; Patey, G. N. A Molecular Mechanism of Ice Nucleation on Model AgI Surfaces. *J. Phys. Chem. B* **2015**, *119*, 9049−9055.
(14) Fitzner, M.; Sosso, G. C.; Cox, S. J.; Michaelides, A. The Many Faces of Heterogeneous Ice Nucleation: Interplay between Surface Morphology and Hydrophobicity. *J. Am. Chem. Soc.* **2015**, *137*, 13658−13669.
(15) Zielke, S. A.; Bertram, A. K.; Patey, G. N. Simulations of Ice Nucleation by Model AgI Disks and Plates. *J. Phys. Chem. B* **2016**, *120*, 2291−2299.
(16) Russo, J.; Tanaka, H. Crystal Nucleation as the Ordering of Multiple Order Parameters. *J. Chem. Phys.* **2016**, *145*, 211801.
(17) Sosso, G. C.; Tribello, G. A.; Zen, A.; Pedevilla, P.; Michaelides, A. Ice Formation on Kaolinite: Insights from Molecular Dynamics Simulations. *J. Chem. Phys.* **2016**, *145*, 211927.
(18) Bi, X.; Cao, B.; Li, T. Enhanced Heterogeneous Ice Nucleation by Special Surface Geometry. *Nat. Commun.* **2017**, *8*, 15372.
(19) Arai, S.; Tanaka, H. Surface-Assisted Single-Crystal Formation of Charged Colloids. *Nat. Phys.* **2017**, *13*, 503−509.
(20) Desgranges, C.; Delhommelle, J. Unusual Crystallization Behavior Close to the Glass Transition. *Phys. Rev. Lett.* **2018**, *120*, 115701.
(21) Sear, R. P. The Non-Classical Nucleation of Crystals: Microscopic Mechanisms and Applications to Molecular Crystals, Ice and Calcium Carbonate. *Int. Mater. Rev.* **2012**, *57*, 328−356.
(22) Jacobson, L. C.; Hujo, W.; Molinero, V. Thermodynamic Stability and Growth of Guest-Free Clathrate Hydrates: A Low-Density Crystal Phase of Water. *J. Phys. Chem. B* **2009**, *113*, 10298−10307.
(23) Falenty, A.; Hansen, T. C.; Kuhs, W. F. Formation and Properties of Ice XVI Obtained by Emptying a Type sII Clathrate Hydrate. *Nature* **2014**, *516*, 231−233.
(24) Sloan, E. D., Jr. Fundamental Principles and Applications of Natural Gas Hydrates. *Nature* **2003**, *426*, 353−359.
(25) Florusse, L. J.; Peters, C. J.; Schoonman, J.; Hester, K. C.; Koh, C. A.; Dec, S. F.; Marsh, K. N.; Sloan, E. D. Stable Low-Pressure Hydrogen Clusters Stored in a Binary Clathrate Hydrate. *Science* **2004**, *306*, 469−471.
(26) Lee, H.; Lee, J.; Kim, D. Y.; Park, J.; Seo, Y.-T.; Zeng, H.; Moudrakovski, I. L.; Ratcliffe, C. I.; Ripmeester, J. A. Tuning Clathrate Hydrates for Hydrogen Storage. *Nature* **2005**, *434*, 743−746.
(27) Wadham, J. L.; Arndt, S.; Tulaczyk, S.; Stibal, M.; Tranter, M.; Telling, J.; Lis, G. P.; Lawson, E.; Ridgwell, A.; Dubnick, A.; Sharp, M. J.; Anesio, A. M.; Butler, C. E. H. Potential Methane Reservoirs beneath Antarctica. *Nature* **2012**, *488*, 633−637.
(28) Berndt, C.; Feseker, T.; Treude, T.; Krastel, S.; Liebetrau, V.; Niemann, H.; Bertics, V. J.; Dumke, I.; Dünnbier, K.; Ferré, B.; Graves, C.; Gross, F.; Hissmann, K.; Hühnerbach, V.; Krause, S.; Lieser, K.; Schauer, J.; Steinle, L. Temporal Constraints on Hydrate-Controlled Methane Seepage off Svalbard. *Science* **2014**, *343*, 284−287.
(29) Widmer-Cooper, A.; Harrowell, P.; Fynewever, H. How Reproducible Are Dynamic Heterogeneities in a Supercooled Liquid? *Phys. Rev. Lett.* **2004**, *93*, 135701.
(30) Widmer-Cooper, A.; Perry, H.; Harrowell, P.; Reichman, D. R. Irreversible Reorganization in a Supercooled Liquid Originates from Localized Soft Modes. *Nat. Phys.* **2008**, *4*, 711−715.
(31) Rozmanov, D.; Kusalik, P. G. Isoconfigurational Molecular Dynamics Study of the Kinetics of Ice Crystal Growth. *Phys. Chem. Chem. Phys.* **2012**, *14*, 13010−13018.
(32) Lupi, L.; Hudait, A.; Peters, B.; Grünwald, M.; Mullen, R. G.; Nguyen, A. H.; Molinero, V. Role of Stacking Disorder in Ice Nucleation. *Nature* **2017**, *551*, 218−222.
(33) Bi, Y.; Porras, A.; Li, T. Free Energy Landscape and Molecular Pathways of Gas Hydrate Nucleation. *J. Chem. Phys.* **2016**, *145*, 211909.
(34) Guo, G.-J.; Zhang, Y.-G.; Li, M.; Wu, C.-H. Can the Dodecahedral Water Cluster Naturally Form in Methane Aqueous Solutions? A Molecular Dynamics Study on the Hydrate Nucleation Mechanisms. *J. Chem. Phys.* **2008**, *128*, 194504.
(35) Guo, G.-J.; Zhang, Y.-G.; Liu, C.-J.; Li, K.-H. Using the Face-Saturated Incomplete Cage Analysis to Quantify the Cage Compositions and Cage Linking Structures of Amorphous Phase Hydrates. *Phys. Chem. Chem. Phys.* **2011**, *13*, 12048−12057.
(36) Barnes, B. C.; Beckham, G. T.; Wu, D. T.; Sum, A. K. Two-Component Order Parameter for Quantifying Clathrate Hydrate Nucleation and Growth. *J. Chem. Phys.* **2014**, *140*, 164506.
(37) Davidson, D. W.; Handa, Y. P.; Ratcliffe, C. I.; Tse, J. S.; Powell, B. M. The Ability of Small Molecules to Form Clathrate Hydrates of Structure II. *Nature* **1984**, *311*, 142−143.

DOI: 10.1021/acs.jpclett.8b03115
J. Phys. Chem. Lett. 2018, 9, 6991−6998

(38) Jacobson, L. C.; Hujo, W.; Molinero, V. Amorphous Precursors in the Nucleation of Clathrate Hydrates. *J. Am. Chem. Soc.* **2010**, *132*, 11806−11811.
(39) Jacobson, L. C.; Hujo, W.; Molinero, V. Nucleation Pathways of Clathrate Hydrates: Effect of Guest Size and Solubility. *J. Phys. Chem. B* **2010**, *114*, 13796−13807.
(40) Sarupria, S.; Debenedetti, P. G. Homogenous Nucleation of Methane Hydrate in Microsecond Molecular Dynamics Simulations. *J. Phys. Chem. Lett.* **2012**, *3*, 2942−2947.
(41) Lauricella, M.; Meloni, S.; Liang, S.; English, N. J.; Kusalik, P. G.; Ciccotti, G. Clathrate Structure-Type Recognition: Application to Hydrate Nucleation and Crystallization. *J. Chem. Phys.* **2015**, *142*, 244503.
(42) Zhang, Z.; Walsh, M. R.; Guo, G.-J. Microcanonical Molecular Simulations of Methane Hydrate Nucleation and Growth: Evidence that Direct Nucleation to sI Hydrate Is among the Multiple Nucleation Pathways. *Phys. Chem. Chem. Phys.* **2015**, *17*, 8870−8876.
(43) Hall, K. Wm.; Carpendale, S.; Kusalik, P. G. Evidence from Mixed Hydrate Nucleation for a Funnel Model of Crystallization. *Proc. Natl. Acad. Sci. U. S. A.* **2016**, *113*, 12041−12046.
(44) Eisen, M. B.; Spellman, P. T.; Brown, P. O.; Botstein, D. Cluster Analysis and Display of Genome-Wide Expression Patterns. *Proc. Natl. Acad. Sci. U. S. A.* **1998**, *95*, 14863−14868.
(45) Haji-Akbari, A.; Debenedetti, P. G. Direct Calculation of Ice Homogeneous Nucleation Rate for a Molecular Model of Water. *Proc. Natl. Acad. Sci. U. S. A.* **2015**, *112* (34), 10582−10588.
(46) Van Driessche, A. E. S.; Van Gerven, N.; Bomans, P. H. H.; Joosten, R. R. M.; Friedrich, H.; Gil-Carton, D.; Sommerdijk, N. A. J. M.; Sleutel, M. Molecular Nucleation Mechanisms and Control Strategies for Crystal Polymorph Selection. *Nature* **2018**, *556*, 89−93.
(47) Allen, R. J.; Warren, P. B.; ten Wolde, P. R. Sampling Rare Switching Events in Biochemical Networks. *Phys. Rev. Lett.* **2005**, *94*, 018104.
(48) Allen, R. J.; Frenkel, D.; ten Wolde, P. R. Simulating Rare Events in Equilibrium or Nonequilibrium Stochastic Systems. *J. Chem. Phys.* **2006**, *124*, 024102.
(49) DeFever, R. S.; Sarupria, S. Nucleation Mechanism of Clathrate Hydrates of Water-Soluble Guest Molecules. *J. Chem. Phys.* **2017**, *147*, 204503.
(50) Haji-Akbari, A.; Debenedetti, P. G. Computational Investigation of Surface Freezing in a Molecular Model of Water. *Proc. Natl. Acad. Sci. U. S. A.* **2017**, *114* (13), 3316−3321.
(51) Haji-Akbari, A. Forward-Flux Sampling with Jumpy Order Parameters. *J. Chem. Phys.* **2018**, *149*, 072303.
(52) Safarik, D. J.; Mullins, C. B. The Nucleation Rate of Crystalline Ice in Amorphous Solid Water. *J. Chem. Phys.* **2004**, *121* (12), 6003−6010.
(53) Laksmono, H.; McQueen, T. A.; Sellberg, J. A.; Loh, N. D.; Huang, C.; Schlesinger, D.; Sierra, R. G.; Hampton, C. Y.; Nordlund, D.; Beye, M.; et al. Anomalous Behaviour of the Homogeneous Ice Nucleation Rate in "No-Man's Land. *J. Phys. Chem. Lett.* **2015**, *6* (14), 2826−2832.
(54) Amaya, A. J.; Pathak, H.; Modak, V. P.; Laksmono, H.; Loh, N. D.; Sellberg, J. A.; Sierra, R. G.; McQueen, T. A.; Hayes, M. J.; Williams, G. J.; et al. How Cubic Can Ice Be? *J. Phys. Chem. Lett.* **2017**, *8* (14), 3216−3222.
(55) Amaya, A. J.; Wyslouzil, B. E. Ice Nucleation Rates near ∼ 225 K. *J. Chem. Phys.* **2018**, *148*, 084501.
(56) Kumar, A.; Nguyen, A. H.; Okumu, R.; Shepherd, T. D.; Molinero, V. Could Mesophases Play a Role in the Nucleation and Polymorph Selection of Zeolites? *J. Am. Chem. Soc.* **2018**, *140*, 16071.

DOI: 10.1021/acs.jpclett.8b03115
J. Phys. Chem. Lett. 2018, 9, 6991−6998